Geomagnetic excursions and paleointensities in the Matuyama Chron at Ocean Drilling Program Sites 983 and 984 (Iceland Basin)

J.E.T. Channell, A. Mazaud, P. Sullivan, S. Turner, M.E. Raymo

JOURNAL OF GEOPHYSICAL RESEARCH, VOL. 107, NO. B6, 2114, 10.1029/2001JB000491, 2002

Geomagnetic excursions and paleointensities in the Matuyama Chron at Ocean Drilling Program Sites 983 and 984 (Iceland Basin)

J. E. T. Channell,[1] A. Mazaud,[2] P. Sullivan,[1] S. Turner,[1] and M. E. Raymo[3]

Received 28 February 2001; revised 27 August 2001; accepted 27 September 2001; published 13 June 2002.

[1] We report natural remanent magnetization (NRM) directions and geomagnetic paleointensity proxies for part of the Matuyama Chron (0.9–2.2 Ma interval) from two sites located on sediment drifts in the Iceland Basin. At Ocean Drilling Program Sites 983 and 984, mean sedimentation rates in the late Matuyama Chron are 15.9 and 11.5 cm kyr^{-1}, respectively. For the older part of the record (>1.2 Ma), oxygen isotope data are too sparse to provide the sole basis for age model construction. The resemblance of the volume susceptibility record and a reference δ^{18}O record led us to match the two records to derive the age models. This match, based on Site 983/984 susceptibility, is consistent with available Site 983/984 benthic δ^{18}O data. Paleointensity proxies were derived from the slope of the NRM versus anhysteretic remanent magnetization plot for alternating field demagnetization in the 30–60 mT peak field range. Paleointensity lows correspond to polarity reversals at the limits of the Jaramillo, Olduvai, Cobb Mountain, and Réunion Subchrons and to seven excursions in NRM component directions. Magnetic excursions (defined here by virtual geomagnetic polar latitudes crossing the virtual geomagnetic equator) are observed at 932, 1048, 1115, 1190–1215 (Cobb Mountain Subchron), 1255, 1472–1480, 1567–1575 (Gilsa Subchron), and 1977 ka. The results indicate that geomagnetic directional excursions, associated with paleointensity minima, are a characteristic of the Matuyama Chron and probably of polarity chrons in general. *INDEX TERMS:* 1520 Geomagnetism and Paleomagnetism: Magnetostratigraphy; 1513 Geomagnetism and Paleomagnetism: Geomagnetic excursions; 1535 Geomagnetism and Paleomagnetism: Reversals (process, timescale, magnetostratigraphy); 1521 Geomagnetism and Paleomagnetism: Paleointensity; *KEYWORDS:* Paleomagnetism, paleointensity, Matuyama Chron, excursions

1. Introduction

[2] Ocean Drilling Program (ODP) Sites 983 (61.4°N, 24.1°W) and 984 (60.4°N, 23.6°W) are located on the Gardar and Bjorn Drifts in the Iceland Basin (Figure 1). Cores from three to four holes at each site were spliced together to produce composite sections without apparent hiatuses [*Shipboard Scientific Party*, 1996a, 1996b]. The composite sections extended into the Olduvai Subchron (to ~1.9 Ma) and Réunion Subchron (to ~2.15 Ma) at Sites 983 and 984, respectively. Mean sedimentation rates in the 12–16 cm kyr^{-1} range have led to paleomagnetic and isotopic records that are among the most detailed for the last 2 Myr. Since 1997, several papers have dealt with different aspects of the paleomagnetic and isotopic records from ODP Sites 983 and 984. *Channell and Lehman* [1997] documented the distribution of virtual geomagnetic poles (VGPs) for the Matuyama-Brunhes boundary and for the young end of the Jaramillo Subchron at Sites 983 and 984. *Mazaud and Channell* [1999] documented the polarity transition record at the top of the Olduvai Subchronozone at Site 983. Integrated paleomagnetic and isotopic records are available for the last 500 kyr from Sites 983 and 984 [*Channell et al.*, 1997, 1998; *Channell*, 1999]. The pre-500 ka paleomagnetic and isotopic record at Site 983 has been documented for the 725–1150 ka interval [*Channell and Kleiven*, 2000] and the 500–725 ka interval [*Channell et al.*, 1998]. *Channell et al.* [1998] were concerned with the paleointensity record (only) and did not deal with the directional paleomagnetic record. In addition to the paleomagnetic/isotopic studies cited above, ODP Leg 162 sites from the Iceland Basin (Sites 980–984) have yielded some of the most detailed Quaternary paleoceanographic records for the North Atlantic [e.g., *Raymo et al.*, 1998; *Oppo et al.*, 1998; *McManus et al.*, 1999; *Venz et al.*, 1999; *Flower et al.*, 2000].

[3] Here we report paleomagnetic directional and paleointensity records for the 0.9–2.2 Ma interval at Site 984

[1]Department of Geological Sciences, University of Florida, Gainesville, Florida, USA.
[2]Laboratoire des Sciences du Climat et de l'Environnement, Gif-sur-Yvette, France.
[3]Department of Earth Sciences, Boston University, Boston, Massachusetts, USA.

0148-0227/02/2001JB000491$09.00

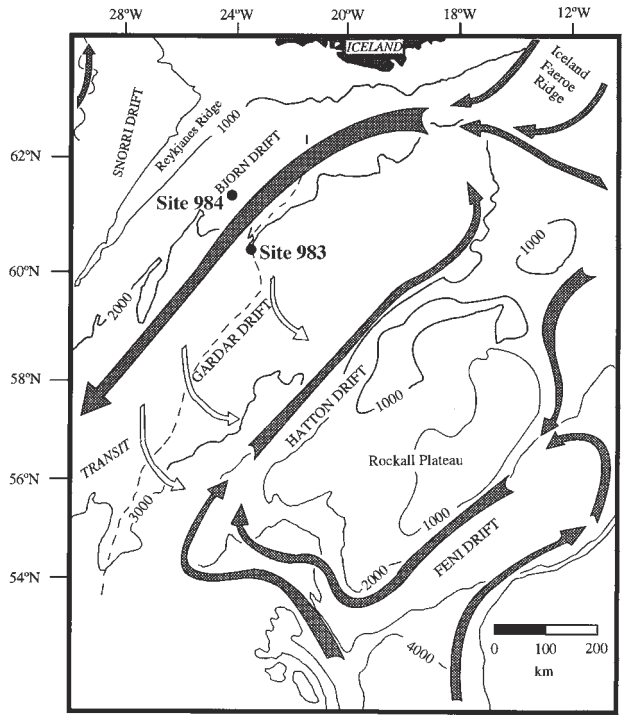

Figure 1. Location map for ODP Sites 983 and 984. Bathymetry is in meters. Dashed line indicates crest of Gardar Drift. Arrows indicate inferred bottom current flows (after *Manley and Caress* [1994] and *McCave et al.* [1980]).

and the 0.9–1.9 Ma interval at Site 983. The magnetic data were acquired from U channel samples collected from the composite sections at the two sites. U channel samples constitute continuous sampling of core sections and typically have 1.5 m length and a square 2 × 2 cm cross section [see *Tauxe et al.*, 1983]. Mean sedimentation rates for the sampled intervals at Sites 983 and 984 are 15.9 and 11.5 cm kyr^{-1}, respectively. The mean sedimentation rates in the Matuyama Chron are approximately twice the mean Matuyama sedimentation rates at Deep Sea Drilling Project (DSDP) Site 609 (~7 cm kyr^{-1}) which up to now have provided the most detailed paleomagnetic records of the Matuyama Chron [*Clement and Robinson*, 1987; *Clement and Kent*, 1987].

[4] The two principal normal polarity subchrons within the mainly reverse polarity Matuyama Chron (0.78–2.56 Ma) were recognized in the 1960s. The Jaramillo and Olduvai Subchrons were first documented by *Doell and Dalrymple* [1966] and *Grommé and Hay* [1963], respectively. Two short intervals of normal polarity prior to the Olduvai were identified in seafloor spreading anomalies by *Heirtzler et al.* [1968] and were named the Réunion Event by *Grommé and Hay* [1971]. *Baksi et al.* [1993] gave a mean $^{40}Ar/^{39}Ar$ age of 2.14 Ma for the Réunion Event on the island of La Réunion. The subchron occurs as a single normal polarity subchron at Site 609 and several other DSDP Leg 94 sites [*Clement and Robinson*, 1987], where it correlated to marine isotope stage (MIS) 79–80 [*Raymo et al.*, 1989].

[5] Although other normal polarity intervals within the Matuyama Chron have been advocated, mainly from iso-

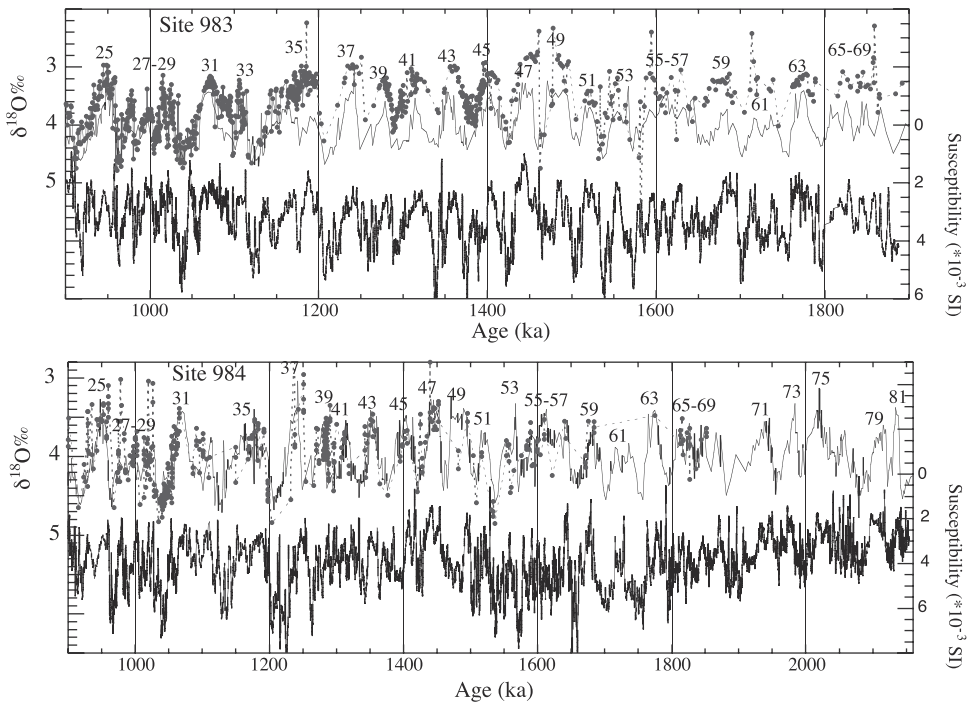

Figure 2. Site 983/984 benthic $\delta^{18}O$ data (solid circles) with the benthic $\delta^{18}O$ record from ODP Site 677 (solid line) [*Shackleton et al.*, 1990] and volume magnetic susceptibility from Sites 983/984 measured in U channel samples. Site 983 $\delta^{18}O$ data are from *Channell and Kleiven* [2000], *Raymo et al.* [1998], and *McIntyre et al.* [1999].

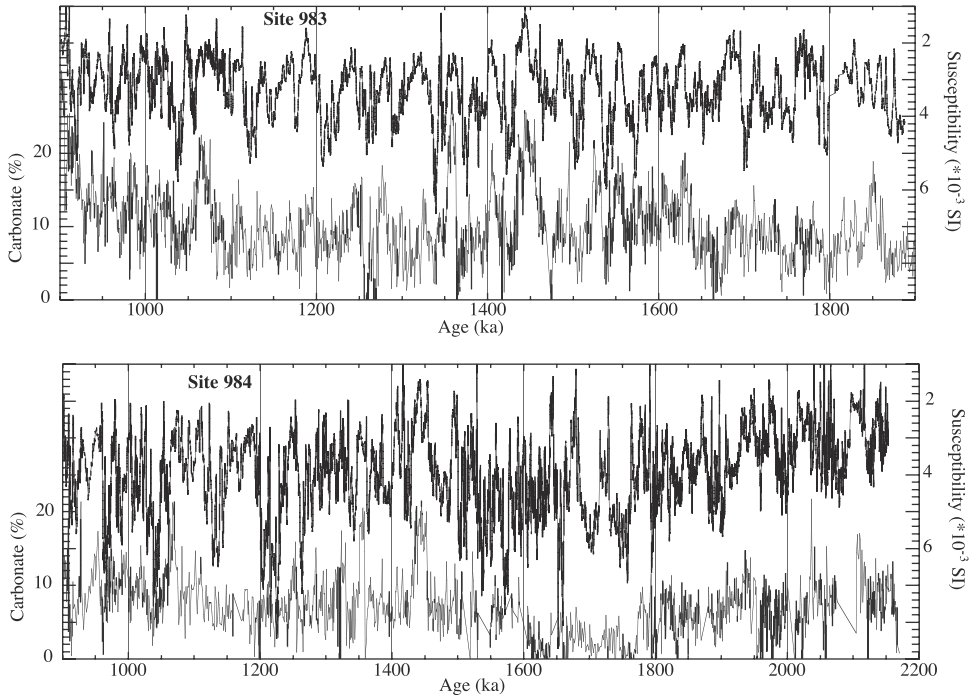

Figure 3. Comparison of Site 983/984 volume magnetic susceptibility (κ) with percentage carbonate determined from reflectance data [*Ortiz et al.*, 1999].

lated excursional directions in volcanic rocks, none of them "stuck" (to the polarity timescale) until the records from DSDP Leg 94 revealed unequivocal evidence for two normal polarity subchrons between the Jaramillo and Olduvai Subchrons [*Clement and Kent*, 1987; *Clement and Martinson*, 1992]. These were labeled the Cobb Mountain and Gilsa Subchrons, inheriting names from studies of volcanic rocks of similar age from California and Iceland,

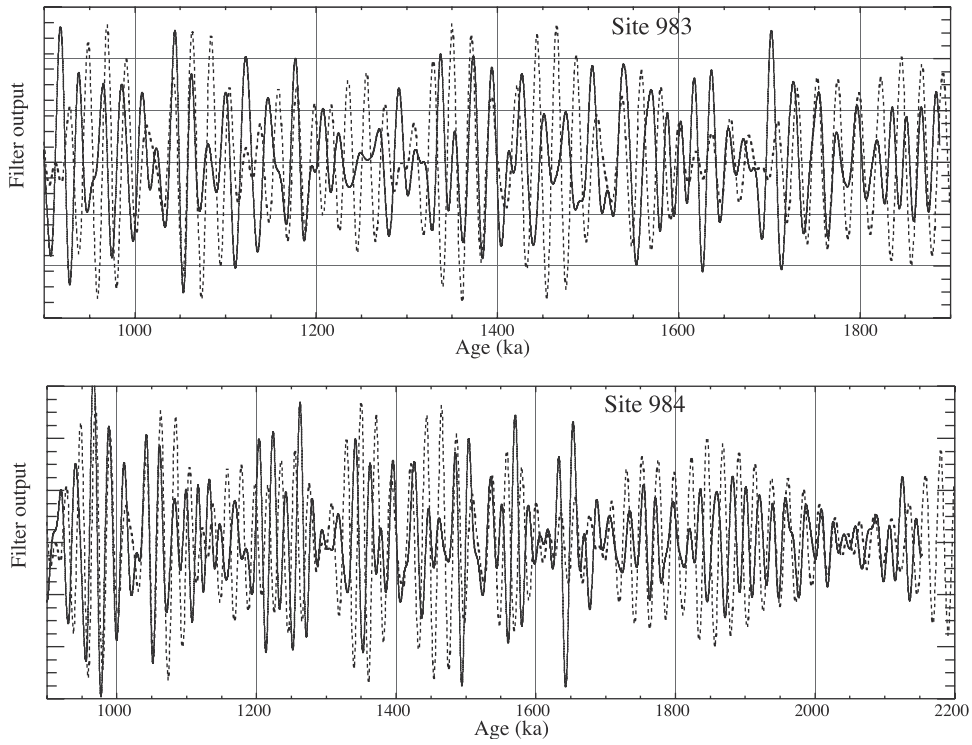

Figure 4. The output of a Gaussian filter centered at 0.05 kyr^{-1} (20-kyr period) with a 0.02 kyr^{-1} band-pass applied to the susceptibility record (solid line) compared with the orbital solution for precession from *Berger and Loutre* [1991] (dashed line).

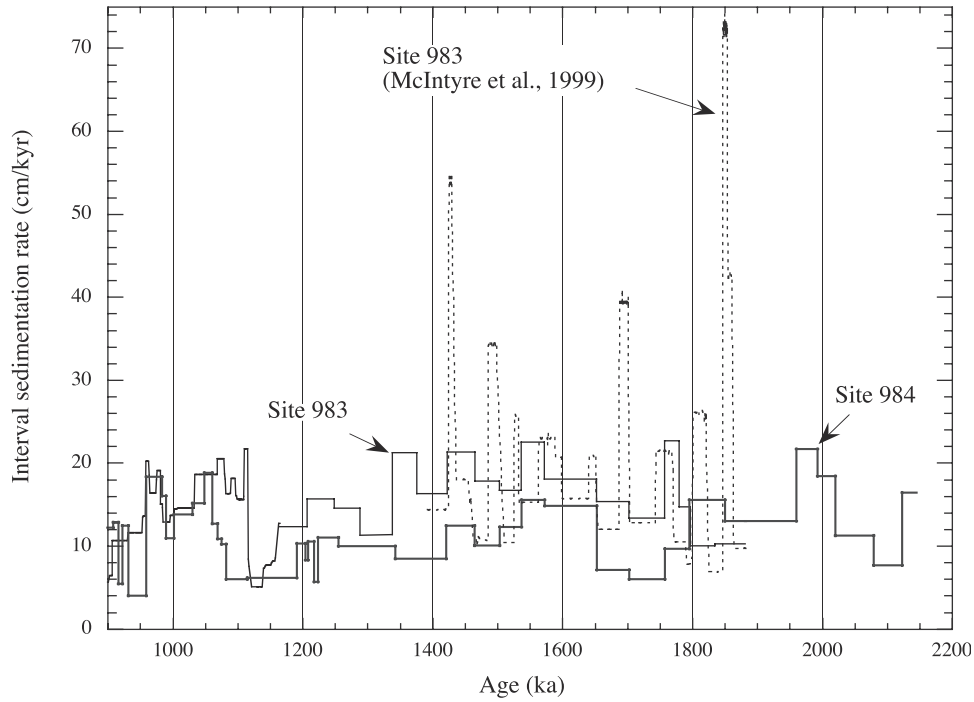

Figure 5. Sedimentation rates the Site 983 (thin solid line) and Site 984 (thick solid line), compared with the Site 983 age model for the 1.4–1.9 Ma interval from *McIntyre et al.* [1999] (dashed line).

respectively, in which excursional directions had been documented [*Mankinen et al.*, 1978; *Watkins et al.*, 1975].

2. Oxygen Isotope Data and Age Models

[6] At Sites 983 and 984, benthic oxygen isotope measurements were made on benthic foraminifera, using specimens of *Cibicidoides wuellerstorfi* and *C. kullenbergi* selected from the >150 μm size fraction of samples collected from the composite sections. For Site 983, benthic $\delta^{18}O$ records have been reported for the 0.9–1.2, 1.2–1.4, and 1.4–1.9 Ma intervals by *Channell and Kleiven* [2000], *Raymo et al.* [1998], and *McIntyre et al.* [1999], respectively. The Site 984 benthic $\delta^{18}O$ data are reported here for the first time and were generated in the stable isotope laboratory at the Massachusetts Institute of Technology. Analytical precision is better than ±0.1‰. Isotope data were calibrated using the National Institute of Standards and Technology (NBS) 19 standard, and values are reported relative to PDB.

[7] The resolution of the benthic oxygen isotope records at Sites 983/984 decreases with age (Figure 2), largely because of the decreasing abundance of foraminifera. Apart from the 0.9–1.2 Ma interval at Sites 983 and 984, where the resolution of the isotope records is relatively high, it is not possible to base the age models on the isotope records alone. We adopt the age model given by *Channell and Kleiven* [2000] for the 0.9–1.2 ka interval at Site 983. For other intervals we exploit the strong resemblance of the susceptibility record with the reference (benthic) $\delta^{18}O$ record from ODP Site 677 [*Shackleton et al.*, 1990] and construct the age models by matching the volume susceptibility to the Site 677 $\delta^{18}O$ record (Figure 2). We chose the Site 677 isotope record because it has high resolution and a robust orbitally tuned chronology [*Shackleton et al.*, 1990].

[8] The volume susceptibility for Sites 983/984 was determined at 1-cm intervals on U channel samples using susceptibility tracks designed for U channels located at the University of Florida and at Gif-sur-Yvette (France). The susceptibility pick-up coils on the two measurement tracks have similar characteristics with Gaussian-shaped response functions of ~3 cm width at half height. The measurement of susceptibility on U channel samples offers superior resolution to ODP shipboard susceptibility measurements on whole core sections, and avoids problems associated with deformation and contamination of sediment close to the core liner.

[9] The susceptibility records at Sites 983 and 984 are better matched to the reference $\delta^{18}O$ record than they are to the carbonate records (Figure 3), indicating that the susceptibility records are not produced entirely by carbonate dilution. The close resemblance of the susceptibility record to the benthic $\delta^{18}O$ record indicates a linkage between global ice volume and bottom current velocity, which influences the abundance of the mineral (magnetite) that produces the susceptibility record in these sediments.

[10] The susceptibility records have power at frequencies corresponding to orbital obliquity and precession. The output of a Gaussian filter centered at 0.05 kyr^{-1} (20 kyr period) with a 0.02 kyr^{-1} band-pass applied to the susceptibility record can be compared with the orbital solution for precession (Figure 4). Although the peak-to-peak match is imperfect, the modulation of orbital precession is well matched by modulation of the filtered susceptibility record (Figure 4). We consider that at least some of the peak-to-peak mismatch is due to noise in the susceptibility record

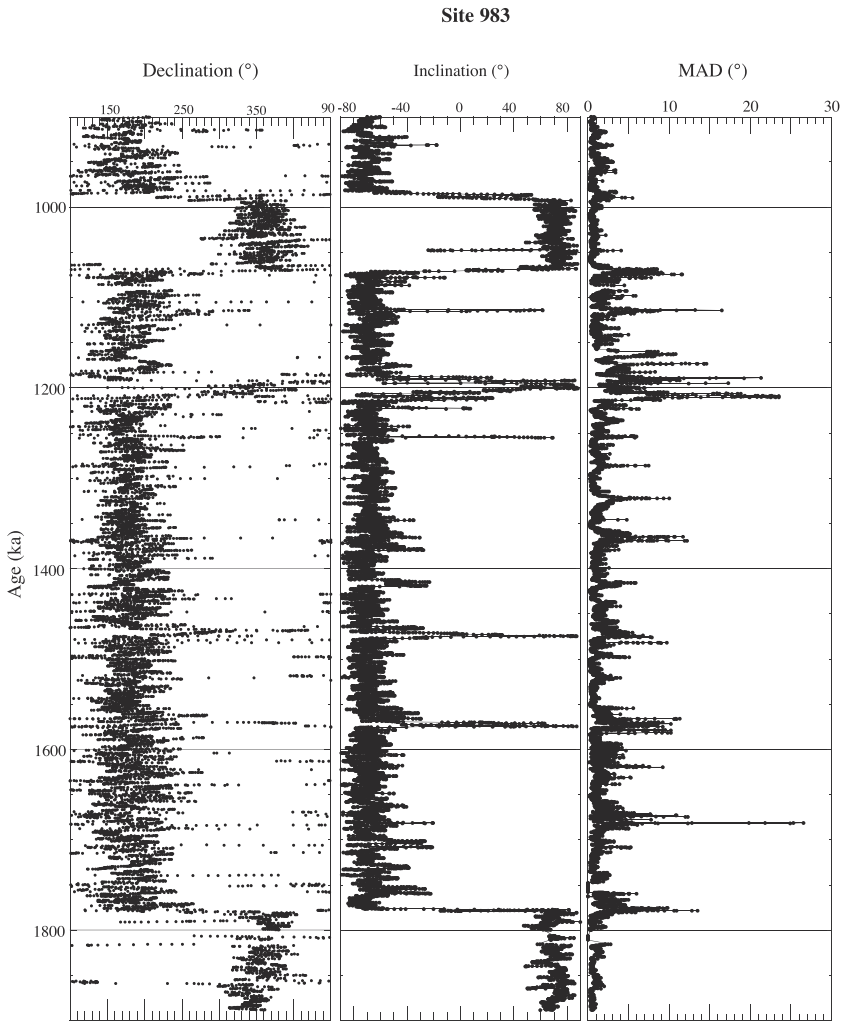

Figure 6. Site 983 component declinations and inclinations and corresponding maximum angular deviation (MAD) values, computed at 1-cm intervals down core for the 30–60 mT demagnetization interval using the standard least squares method.

produced by stochastic influences such as volcanic ash layers. For this reason, and because of unknown lag between precessional forcing and response, we have refrained from tuning of the filtered susceptibility record to the astronomical solution. Nonetheless, the match of the filtered susceptibility records to the astronomical solution for precession strengthens the age model.

[11] The age model produced by matching the volume susceptibility record to the reference (Site 677) $\delta^{18}O$ record is consistent with the available benthic $\delta^{18}O$ from Sites 983/984 (Figure 2). The existence of the Site 983/984 $\delta^{18}O$ data strengthens the supposition that the susceptibility data tracks the reference (ODP Site 677) $\delta^{18}O$ record. The resulting age model yields sedimentation rates in the 4–23 cm kyr^{-1} range (Figure 5). Note the similarity in the long-term change in sedimentation rates at the two sites and the variability in sedimentation rates with changes by a factor of 4 or 5 over intervals of <100 kyr. The age model for Site 983 differs from that given by *McIntyre et al.* [1999] for the 1.4–1.9 Ma interval at this site. *McIntyre et al.* [1999] correlated the benthic $\delta^{18}O$ record to a reference record from ODP Site 659 [*Tiedemann et al.*, 1994]. The sedimentation rates for the *McIntyre et al.* [1999] age model reach 72 cm kyr^{-1}, several times greater than the maximum sedimentation rates advocated here (Figure 5).

3. Magnetic Properties

3.1. Directional Data

[12] During ODP Leg 162, archive halves of core sections from Sites 983/984 were demagnetized at peak fields up to 25 mT using the shipboard pass-through magnetometer [*Channell and Lehman*, 1999]. In conjunction with the determination of the polarity stratigraphy at Sites 983 and 984, stepwise alternating field (AF) demagnetization of discrete samples collected from the working halves of core sections indicated that the characteristic magnetization is isolated at peak demagnetization fields >20 mT [*Channell and Lehman*, 1999]. U channel samples collected postcruise from the archive halves of core sections from the Site 983/984 composite sections were stepwise demagnetized in 5-mT steps for peak fields of 15–60 mT, with additional steps to 120 mT over much of the sampled interval. U channel measurements were made

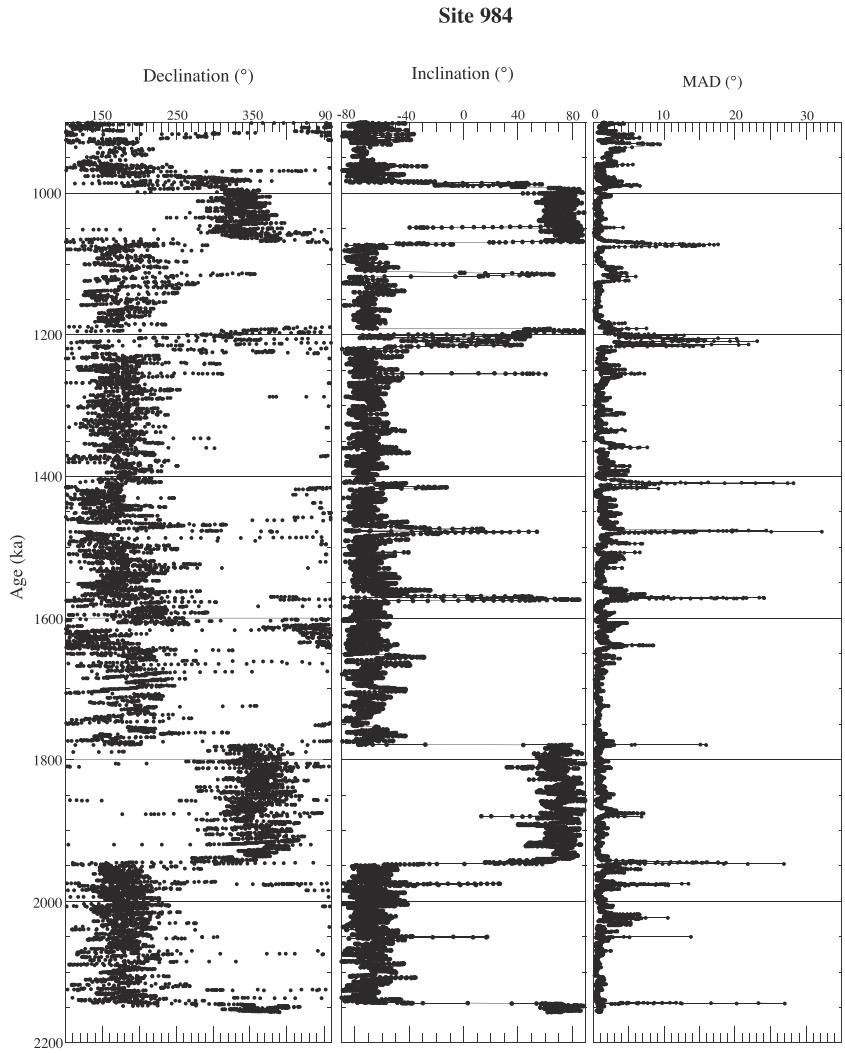

Figure 7. Site 984 component declinations and inclinations and corresponding maximum angular deviation (MAD) values, computed at 1-cm intervals down core for the 30–60 mT demagnetization interval using the standard least squares method.

on 2G Enterprises magnetometers designed to measure U channels at Gif-sur-Yvette (France) and at the University of Florida. Measurements were made at 1-cm intervals, although measurements at this spacing are not independent of each other due to the ~4.5 cm width of the response function of the magnetometer pick-up coils [see *Weeks et al.*, 1993]. The characteristic magnetization component directions were then computed, at 1-cm intervals, for the 30–60 mT demagnetization interval using the standard least squares method [*Kirschvink*, 1980] (Figures 6 and 7). For both Sites 983 and 984 declinations were "corrected" using data from the shipboard core orientation (tensor) tool applied to individual cores. For some cores, tensor data are not available or poor quality, and for these cores the declination correction was performed by rotating individual cores such that the mean core declination is oriented north (360°) in the Brunhes Chron or south (180°) in the reverse polarity intervals of the Matuyama Chron.

[13] The maximum angular deviation (MAD) values are generally <5°, indicating that component directions are usually well-defined (Figures 6 and 7). Higher MAD values are associated with polarity reversals and directional excursions (Figures 6 and 7) where overprinting by the postexcursional or postreversal geomagnetic field compromises the definition of magnetization components. In the vicinity of reversals and excursions, MAD values could have been reduced by choosing a different demagnetization interval (other than the 30–60 mT interval) to define the magnetization component. Inspection of individual orthogonal projections of U channel data in the vicinity of excursions indicates that overprinting by the postexcursional field usually affects a limited depth interval. For example, the excursion at 1115 ka at Site 983 (see Figure 6) shows severely overprinted orthogonal projections close to 138.77 meters composite depth (mcd) (Figure 8), but the normal polarity directions which define the excursion are well defined below this level. At Site 984 the normal polarity directions which define the excursion at 1570 ka (see Figure 7) are also well defined (Figure 9).

[14] To calculate mean inclinations and virtual geomagnetic polar (VGP) dispersions, we use the *Vandamme* [1994] procedure for eliminating excursional and transi-

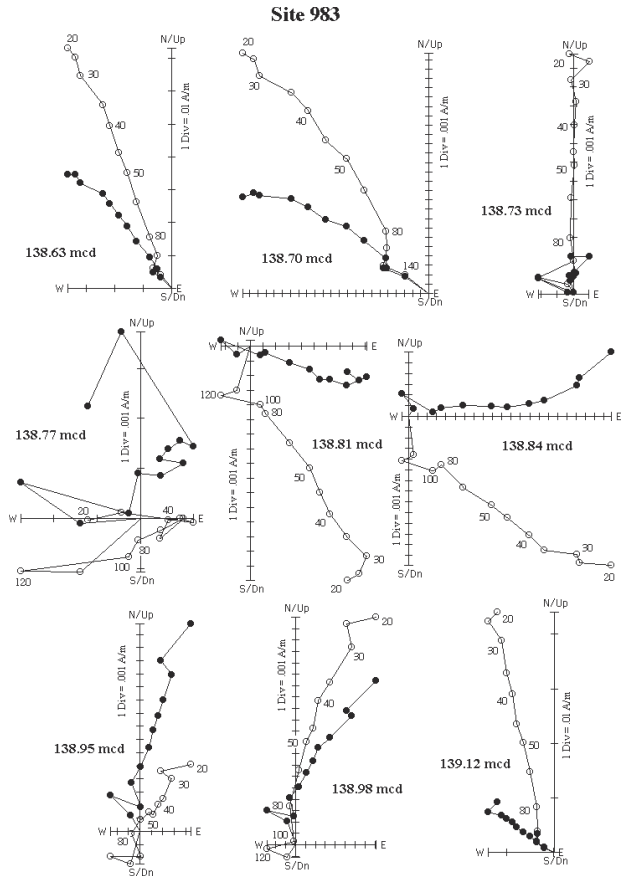

Figure 8. Orthogonal projection of alternating field demagnetization data for samples from Site 983 which record the Punaruu Subchron at 1115 ka (see Figure 6). Open and solid symbols indicate projection on the vertical and horizontal planes, respectively. The position of the sample in meters composite depth (mcd) are indicated. The peak alternating field for some demagnetization steps is indicated in mT.

tional VGPs from the data set. The VGP latitude cutoff values calculated using this procedure are 41° (33°) and 45° (38°) for the Matuyama (Brunhes) Chron at Sites 983 and 984, respectively. The geocentric axial dipole (GAD) inclinations for the Sites 983 and 984 locations are 74.15° and 74.16°, respectively. Mean inclinations for the Brunhes Chron at Sites 983/984 are within 1° of the GAD inclination [see *Channell*, 1999]. The mean inclinations decrease progressively with age in the Matuyama Chron. The inclination flattening reaches 2° for the Olduvai Subchron at Site 984 and 5° for the short interval of the Matuyama Chron prior to the Olduvai. The inclination flattening may have been induced by the coring process as the hydraulic piston corer reached its depth limit in the sediment column. Virtual geomagnetic polar (VGP) dispersions within the Matuyama and Brunhes Chrons at Sites 983/984 (Figure 10) are greater for the Matuyama, and lower for the Brunhes, than those predicted (~19°) by secular variation Model G [*McFadden et al.*, 1988]. This suggests that component magnetization directions in the Matuyama Chron are influenced by (normal polarity) magnetic overprints.

3.2. Paleointensity Data

[15] Paleomagnetic paleointensity proxies in sediments are constructed by dividing (normalizing) the natural remanent magnetization (NRM) intensity by a magnetic parameter sensitive to changes in concentration of magnetic grains. The ideal normalizer activates the same grains as those which carry the NRM, thereby compensating for down core variations in the concentration of remanence carrying grains. Three bulk magnetic parameters have been used as normalizers to produce paleointensity proxies: volume magnetic susceptibility (κ), anhysteretic remanence (ARM), and isothermal remanence (IRM). Susceptibility is not usually selected as it is sensitive to large multidomain magnetite grains (often

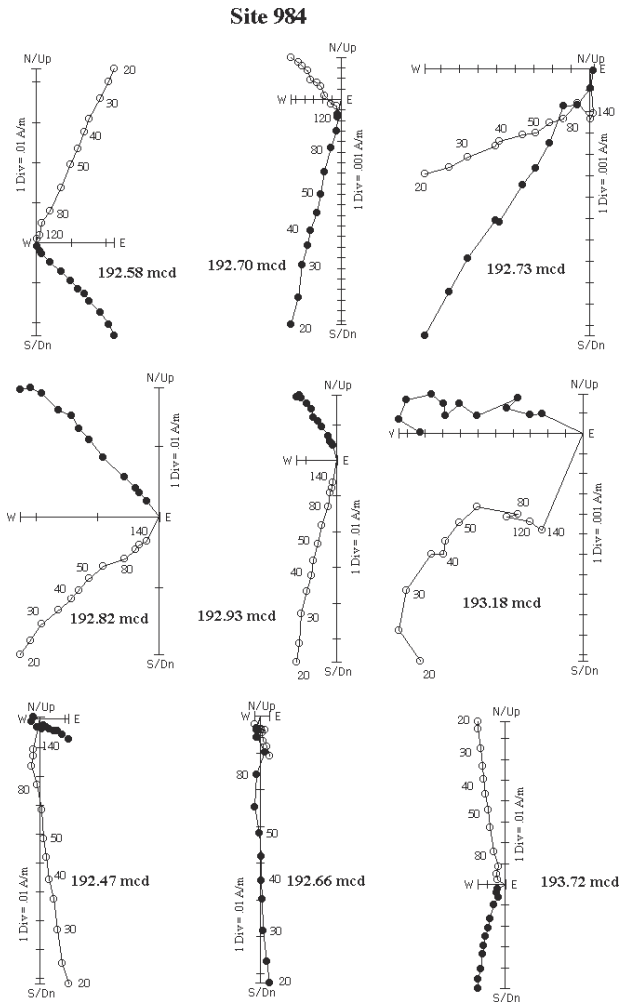

Figure 9. Orthogonal projection of alternating field demagnetization data for samples from Site 984 which record the Gilsa Subchron at 1567–1575 ka (see Figure 7). Open and solid symbols indicate projection on the vertical and horizontal planes, respectively. The position of the sample in meters composite depth (mcd) are indicated. The peak alternating field for some demagnetization steps is indicated in mT.

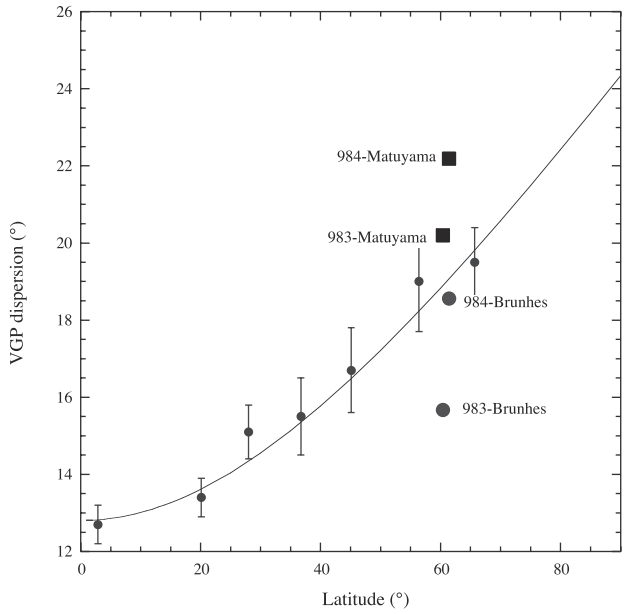

Figure 10. Virtual geomagnetic polar (VGP) dispersion determined from volcanic rocks (with error bars) compared with the secular variation Model G (line) [from *McFadden et al.*, 1988]. The mean VGP dispersions for the Matuyama and Brunhes Chrons at Sites 983/984 are higher and lower, respectively, than predicted by the model.

a constituent of ice rafted debris) as well as small (superparamagnetic) grains, both of which are not important carriers of magnetic remanence. In this study, the ARM was acquired in a 100-mT alternating field with a 0.05-mT DC bias field, and the IRM was acquired in a 500-mT DC field. ARM and IRM were AF demagnetized in the same peak fields as used to demagnetize the NRM and measured at 1-cm intervals down core.

[16] In order to achieve satisfactory normalization, and hence useful paleointensity proxies, the carrier of magnetic remanence in the sediment should be single-domain (SD) or pseudo-single-domain (PSD) magnetite. In addition, the concentration of magnetite, as recorded by bulk magnetic parameters such as susceptibility and ARM, should not vary by more than an order of magnitude [see *King et al.*, 1983; *Tauxe*, 1993]. Coercivity and blocking temperature spectra and hysteresis ratios from previous magnetic studies of Site 983 [*Channell et al.*, 1997, 1998; *Channell and Kleiven*, 2000] and of the 0–500 ka interval at Site 984 [*Channell*, 1999], indicate that PSD magnetite is the principal remanence carrier at both sites. ARM intensities, sensitive to the abundance of remanence-carrying magnetite, vary by less than an order of magnitude down section (Figure 11), consistent with the criteria for paleointensity determinations advocated by *King et al.* [1983] and *Tauxe* [1993]. The plot of anhysteretic susceptibility (κ_{arm}) against susceptibility (κ) provides a useful means of monitoring magnetite grain size. The quasi-linear relationship between κ_{arm} and κ indicates uniform magnetite grain size, apart from in the 1800–2150 ka interval at Site 984 (Figure 12).

[17] The paleointensity record for the 900–1100 ka interval at Site 983 has been previously published [*Channell and Kleiven*, 2000]. For the 1100–1900 ka interval at Site 983 and for the 900–2150 ka interval at Site 984, we use the slope of the NRM intensity versus ARM intensity plot in the 30–60 mT demagnetization interval as the paleointensity proxy. This provides very similar results to using the mean

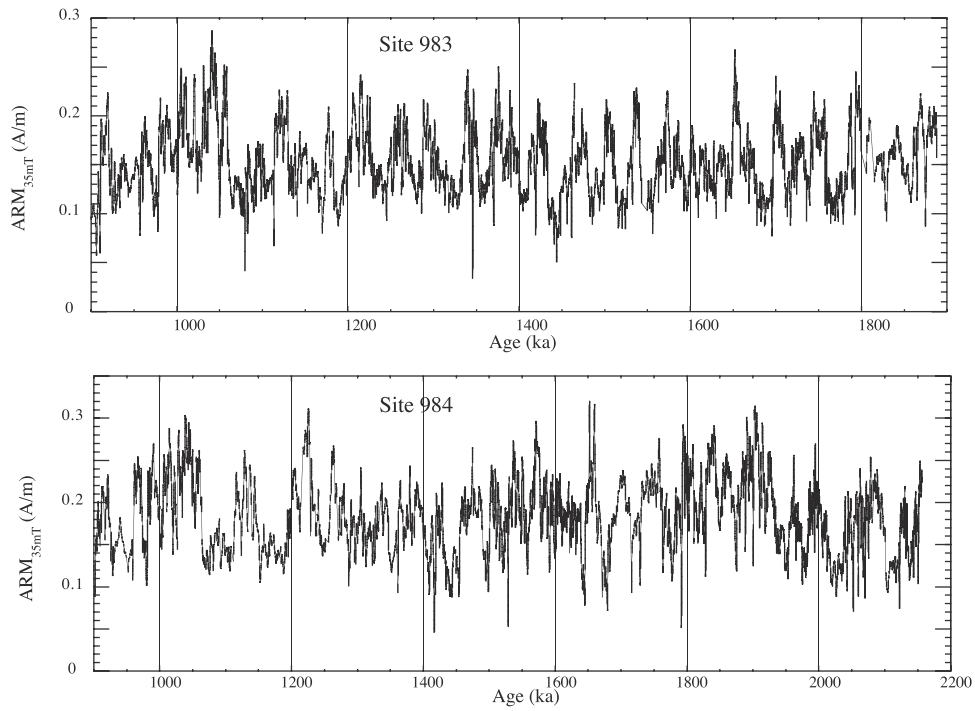

Figure 11. Intensity of anhysteretic remanent magnetization (ARM) after demagnetization at peak fields of 35 mT for Sites 983/984.

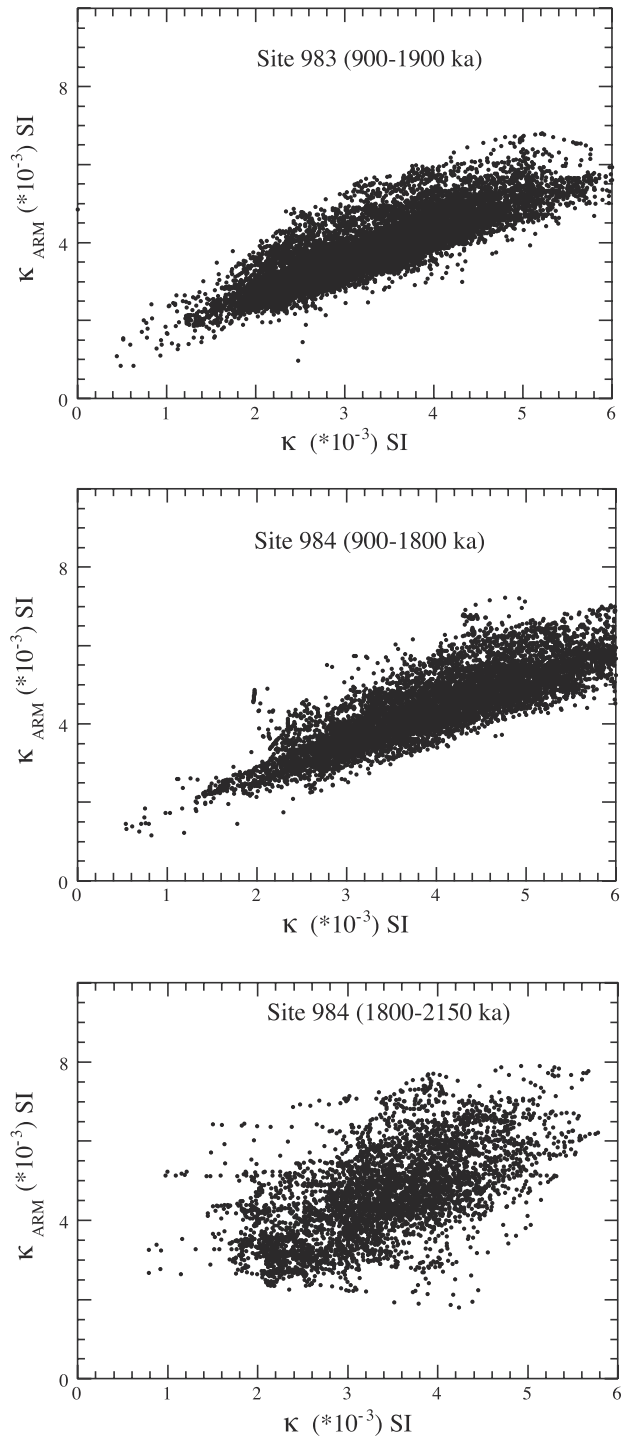

Figure 12. Anhysteretic susceptibility (κ_{arm}) plotted against volume susceptibility for the 900–1900 ka interval at Site 983 and for the 900–1800 ka and 1800–2150 ka intervals at Site 984.

NRM/ARM, calculated for demagnetization steps in the 30–60 mT peak field range. We use the NRM/ARM slope and calculate a linear correlation coefficient (r) to monitor the linearity of the NRM versus ARM plot, each 1-cm down core (Figure 13). Values of r close to unity indicate that the NRM/ARM slope is well defined and that the coercivity of the NRM is a good match to the coercivity of ARM in the 30–60 mT demagnetization range. Hence ARM probably monitors the concentration of NRM-carrying grains and is therefore a valid normalizer for these sediments.

[18] Paleointensity proxies based on NRM/ARM are similar to those based on NRM/IRM. This has been demonstrated for the 700–1100 ka interval at Site 983 [see *Channell and Kleiven*, 2000, Figure 9]. For Site 984, there are differences in amplitude of NRM/ARM and NRM/IRM features, although there is good consistency for each ratio during progressive demagnetization (Figure 14). NRM/IRM and NRM/ARM based paleointensity proxies yield similar results. Our decision to use NRM/ARM rather than NRM/IRM in Figure 13 is based on the perturbing effect of ash-rich layers which have very high IRM intensities, occasionally exceeding the dynamic range of the U channel magnetometer.

[19] The paleointensity records at the two sites are comparable, with paleointensity lows corresponding to polarity reversals or geomagnetic excursions (Figure 13). No systematic paleointensity trend within polarity chrons, such as ''sawtooth'' profiles [*Valet and Meynadier*, 1993], are observed. Also, short-lived postreversal intensity highs, as documented in volcanic records of Kauai [*Bogue*, 2001], are not observed. Paleointensity values appear to recover within a few thousand years of the directional change associated with polarity reversals or geomagnetic excursions.

[20] Several other paleointensity records are available for the 900–1500 ka interval. In Figure 15 we compare the Site 983/984 paleointensity records (here smoothed with a 10-point running mean) with those from the equatorial Pacific [*Valet and Meynadier*, 1993], the equatorial Indian Ocean [*Meynadier et al.*, 1994], the Ontong-Java Plateau [*Kok and Tauxe*, 1999], and the California Margin [*Guyodo et al.*, 1999]. Mean sedimentation rates in the Matuyama Chron at ODP Site 1021 (California Margin) are ~2.5 cm kyr^{-1}, and rates are <2 cm kyr^{-1} for the other records listed above. The age control at ODP Site 1021 (California Margin) for the Matuyama Chron is based on linear interpolation from the Matuyama-Brunhes boundary (MBB) to the boundaries of the Jaramillo Subchron [*Guyodo et al.*, 1999]. The Ontong-Java stack is dated by linear interpolation between polarity reversals at the MBB and the Gauss-Matuyama boundary [*Kok and Tauxe*, 1999]. The age control for the equatorial Pacific Leg 138 record [*Valet and Meynadier*, 1993] is based on orbital tuning of the gamma ray attenuation porosity evaluator (GRAPE) density stratigraphy [*Shackleton et al.*, 1995]. The chronology for the Indian Ocean record [*Meynadier et al.*, 1994] is based on susceptibility correlation to a nearby site (ODP Site 709). Paleointensity lows at 990, 1070, and 1200 ka in Figure 15 correspond to the boundaries of the Jaramillo Subchron and to the Cobb Mountain Subchron. These paleointensity lows are observed in all records. Many other features seen in the Site 983/984 paleointensity records are not seen in the other records (Figure 15). This is not simply related to the lower sedimentation rate at sites other than Sites 983/984, because the Site 983/984 records are smoothed with a 10-point running mean in Figure 15.

4. Conclusions

[21] Correlations of polarity excursions at Sites 983/984 to isotopic stages and absolute ages are shown in Table 1

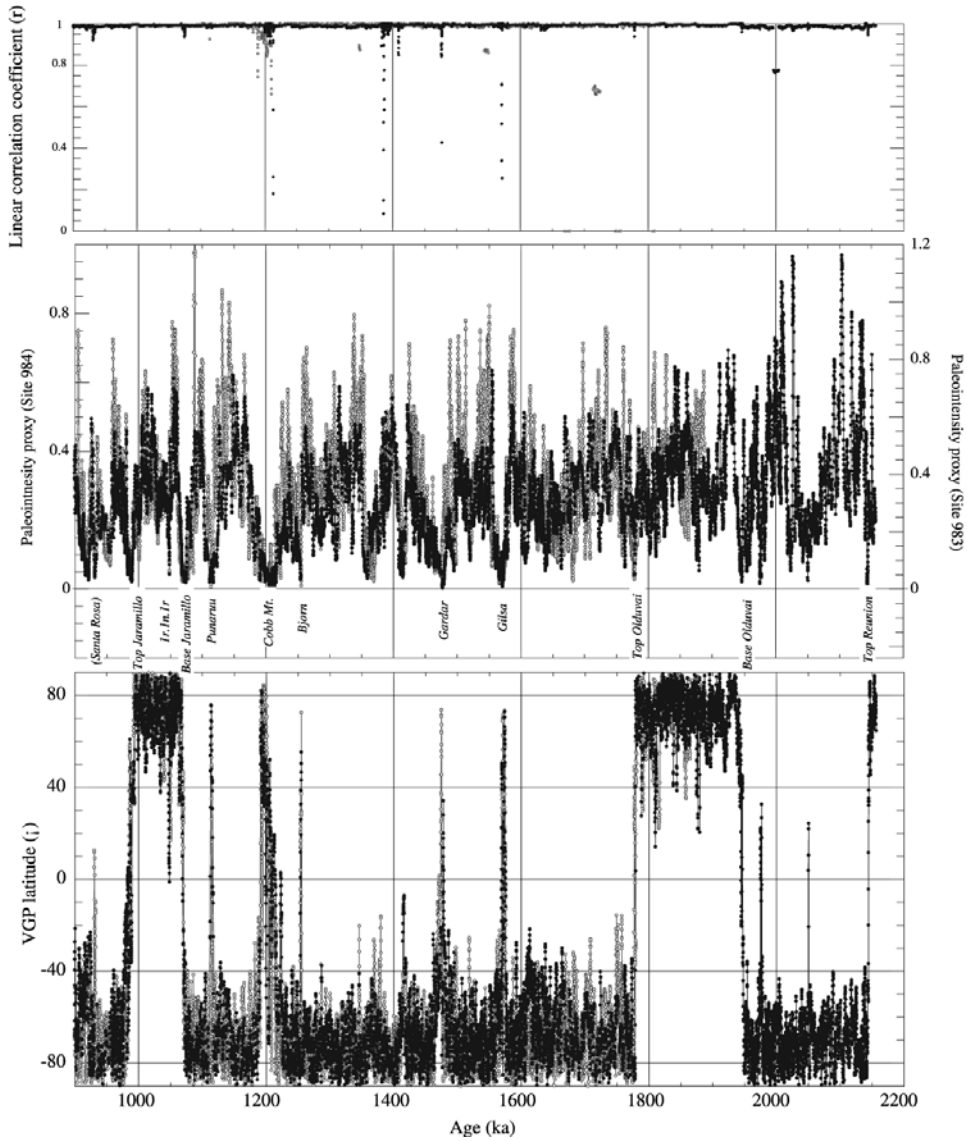

Figure 13. Site 983 (open symbols) and Site 984 (solid symbols) paleointensity proxy based on the slope of the NRM/ARM plot in the 30–60 mT peak demagnetization interval. The linear correlation coefficient (r) indicates the linearity of the NRM/ARM plot in this demagnetization interval. The virtual geomagnetic polar (VGP) latitudes show polarity reversals and geomagnetic excursions (defined here as VGP latitudes which cross the virtual geomagnetic equator) relative to the paleointensity record. See color version of this figure at back of this issue.

and Figure 16. Directional excursions, defined here by virtual geomagnetic polar (VGP) latitudes which cross the virtual geomagnetic equator (Figure 13), are associated with paleointensity lows. *Valet and Meynadier* [1993] noted a similar relationship between excursions and paleointensities in the Brunhes Chron. Although paleomagnetic data from volcanic rocks have indicated numerous geomagnetic excursions within the Brunhes and Matuyama Chrons [*Champion et al.*, 1988; *Singer et al.*, 1999], most are isolated observations and not part of continuous magnetostratigraphic sections. Because of the stochastic nature of volcanic eruption, sedimentary records from the deep sea are generally more continuous than volcanic records. The combination of high sedimentation rate "drift" sites and high-resolution (U channel) sampling provides submillennial measurement resolution and therefore enhances the probability of detecting short geomagnetic excursions.

[22] Prior to the deployment of the hydraulic piston corer (HPC) by the Deep Sea Drilling Project (DSDP) in the early 1980s, records of the Matuyama Chron from deep sea were restricted to sediments with accumulation rates <1 cm kyr^{-1} due to the limited penetration of conventional piston coring devices. The HPC led to the recovery of records of the Matuyama Chron from sediments with accumulation rates in excess of 2 cm kyr^{-1}. At DSDP Site 502 in the Caribbean, the Olduvai Subchron was recorded at 45 m below seafloor using HPC technology [*Kent and Spariosu*, 1983]. At DSDP Site 609 the Olduvai Subchron was recorded at 120 m depth [*Clement and Robinson*, 1987].

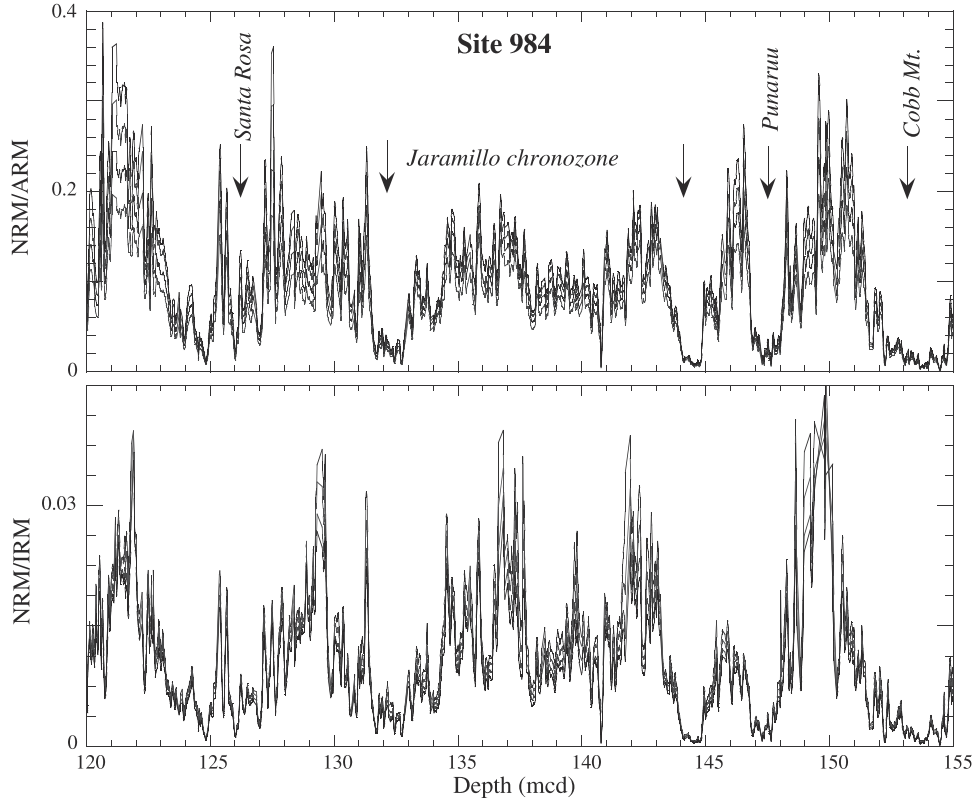

Figure 14. Site 984 normalized remanence values (NRM/ARM and NRM/IRM) after alternating field demagnetization at peak fields of 25, 30, 35, and 40 mT for the 120–155 mcd interval (900–1200 ka).

At Sites 983 and 984 the top of the Olduvai Subchron was recorded at 248 and 215 m, respectively.

[23] The age models described here for Sites 983/984 yield ages for the bounds of the Jaramillo and Olduvai Subchrons (Table 1), which are consistent with astrochronological estimates [*Shackleton et al.*, 1990]. This is not surprising as the Site 983/984 age models are derived by matching the U channel susceptibility record to the orbitally tuned ODP Site 677 record on which the astrochronology of *Shackleton et al.* [1990] is based. Note, however, that there is no magnetic stratigraphy at ODP Site 677. The Site 677 chronology was correlated to subchron boundaries by utilizing the marine isotope stage (MIS) to chron boundary correlation from DSDP Sites

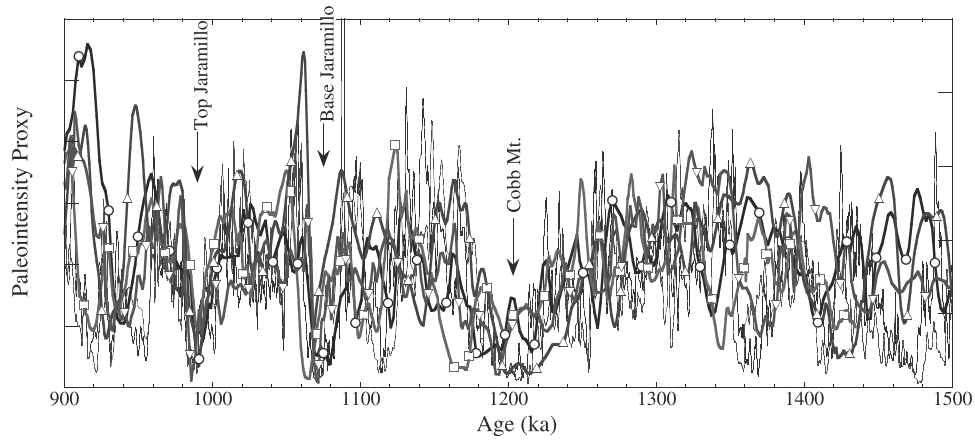

Figure 15. Comparison of the Site 983/984 paleointensity records (smoothed with a 10-point running mean, thin lines) with other published paleointensity records (thick lines). Triangles, Ontong-Java Plateau [*Kok and Tauxe*, 1999]; inverted triangles, equatorial Pacific [*Valet and Meynadier*, 1993]; open circles, equatorial Indian Ocean [*Meynadier et al.*, 1994]; open squares, California Margin [*Guyodo et al.*, 1999]. See color version of this figure at back of this issue.

Table 1. Correlation of Subchron Boundaries and Excursions to Marine Isotopic Stage and Absolute Age

Name of Subchron	Subchron Label[a]	Marine Isotope Stage				Age, ka (This Paper)	Duration, kyr (This Paper)
		Sites 607, 609, 677[b]	Site 659[c]	Italy[d]	This Paper		
Santa Rosa	1r.1r.1n				top 25	932	3
Jaramillo					base 27	987	8
Top	top 1r.1n	mid 27	27				
	1r.1n.1r				base 30	1048	3
Base	base 1r.1n	mid 31	31		base 31	1068	5
Punaruu	1r.2r.1r				mid 34	1115	5
Cobb Mountain							
Top	top 1r.2r.2n	base 35			base 35	1190	
Base	base 1r.2r.2n	base 35			top 37	1215	
Bjorn	1r.2r.3n				top 38	1255	3
Gardar	1r.2r.4n				49	1472–1480	8
Gilsa	1r.2r.5n	53			54	1567–1575	8
Olduvai							
Top	top 2n	base 63	64	64	63	1778	4
Base	base 2n	base 71	72	71	base 71	1945	5
	2r.1r.1n				top 73	1977	3
Réunion top	top 2r.1n	79–80		81	81	2144	3

[a] Nomenclature of *Cande and Kent* [1992].
[b] *Ruddiman et al.* [1989], *Raymo et al.* [1989], and *Shackleton et al.* [1990].
[c] *Tiedemann et al.* [1994].
[d] *Lourens et al.* [1996].

607/609 [*Ruddiman et al.*, 1989; *Raymo et al.*, 1989] and Site 522 [*Shackleton et al.*, 1984]. The MIS correlations to the Jaramillo and Olduvai Subchrons at Sites 983/984 (Table 1) are consistent with the correlations cited above as well as with correlations from Site 659 [*Tiedemann et al.*, 1994] and from sections exposed on land in Italy [*Lourens et al.*, 1996]. The new MIS correlations to other polarity subchrons and geomagnetic events (Table 1) will be testable as more high-resolution records become available.

[24] *Singer et al.* [1999] have reviewed radiometric ages of volcanic rocks recording polarity reversals and geomagnetic excursions in the late Matuyama Chron (Figure 16). On Maui (Hawaiian Islands), a thick (~30 m) sequence of lavas yielding low virtual geomagnetic polar (VGP) latitudes has been dated as spanning the 880–886 ka interval [*Singer et al.*, 1999]. These ages are similar to a group of ages associated with excursional magnetization directions from the Kamikatsura Tuff (Japan), Chinese loess, and basalts in Iceland and the western United States [see *Champion et al.*, 1988; *Takatsugi and Hyodo*, 1995]. Transitional magnetization directions from volcanic rocks at Santa Rosa (New Mexico) have yielded $^{40}Ar/^{39}Ar$ ages [*Izett and Obradovich*, 1994; *Spell and McDougall*, 1992] which give a mean of 922 ka [*Singer et al.*, 1999]. Unlike the records of the Santa Rosa and Kamikatsura subchrons, normal polarity directions from the Punaruu Valley (Tahiti) are found within a relatively continuous volcanic section which includes the Jaramillo Subchronozone [*Chauvin et al.*, 1990]. The so-called Punaruu Event is recorded in several tens of meters of basalt and is stratigraphically below the Jaramillo Subchronozone. It has been dated at 1105 ka by *Singer et al.* [1999] (see Figure 16). This geomagnetic event appears in the sediment record from ODP Site 1021 (California Margin) where an age of 1.1 Ma is based on uniform sedimentation rate between the MBB and the top of the Jaramillo [*Guyodo et al.*, 1999].

[25] *Mankinen et al.* [1978] documented a site of normal polarity in the Alder Creek rhyolite at Cobb Mountain

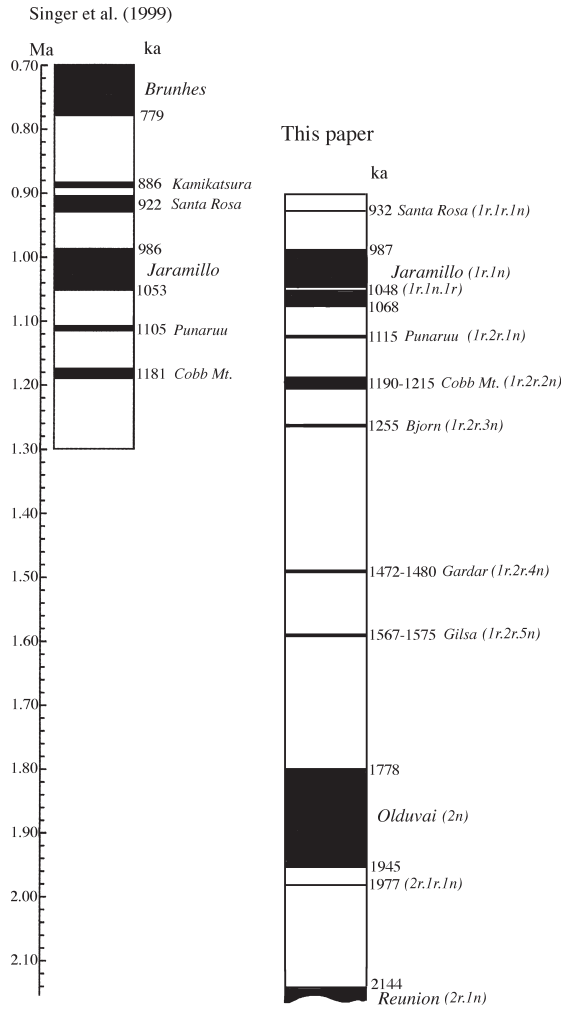

Figure 16. (left) The $^{40}Ar/^{39}Ar$ ages of polarity subchrons/excursions from *Singer et al.* [1999]. (right) Ages of polarity subchrons/excursions based on their identification at Sites 983/984 (see Table 1).

(California) which has yielded an $^{40}Ar/^{39}Ar$ age of 1186 ka [*Turrin et al.*, 1994]. Further work by *Mankinen and Grommé* [1982] in the Cosa Range (California) supported the existence of the Cobb Mountain Subchron. DSDP Site 609 in the central North Atlantic provided the first unequivocal documentation of a normal polarity zone of similar age in deep-sea sediments [*Clement and Kent*, 1987; *Clement and Martinson*, 1992]. At Site 609 the Cobb Mountain Subchron can be correlated to MIS 35 [*Ruddiman et al.*, 1989] (Table 1). This subchron has also been recognized in the southern Labrador Sea [*Clement and Martinson*, 1992], in the Celebes and Sulu Seas [*Hsu et al.*, 1990], in the Lau Basin [*Abrahamsen and Sager*, 1994], on the California Margin [*Guyodo et al.*, 1999], and on the Bermuda Rise [*Yang et al.*, 2001].

[26] *Clement and Kent* [1987] documented a normal polarity subchron older than the Cobb Mountain Subchron and younger than the Olduvai Subchron at DSDP Site 609. They labeled this the Gilsa Subchron, implying a link to the series of polarity zones (from base R-N-R-N) from Iceland called the Gilsa Event by *McDougall and Wensink* [1966]. *Watkins et al.* [1975] restudied the section in Iceland where "Gilsa" was first applied and reported a normal polarity lava yielding a K-Ar age of 1.58 Ma overlying a normal polarity lava with an age of 1.67 Ma. The older lava was associated with the Olduvai Subchron and a younger normal polarity subchron, the Gilsa Subchron. The position of the Gilsa Subchron at DSDP Site 609 [*Clement and Kent*, 1987] is correlated to MIS 53 (1.43 Ma) (Table 1) based on the Site 609 chronology of *Ruddiman et al.* [1989].

[27] At ODP Sites 983 and 984 the mean sedimentation rates within the Matuyama Chron are approximately twice those at DSDP Site 609. In addition, continuous U channel sampling maximizes the measurement resolution. As a result, we see seven geomagnetic excursions, in addition to the Cobb Mountain Subchron, in which VGP latitudes cross the virtual geomagnetic equator (Figure 13). These are at 932, 1048, 1115, 1190–1215 (Cobb Mountain Subchron), 1255, 1472–1480, 1567–1575, and 1977 ka (Table 1 and Figure 16). The excursion at 932 ka is recorded at Site 983 only; however, all others are recorded at both sites. The durations of the Matuyama geomagnetic excursions are estimated to be ~3–8 kyr, comparable with the duration of directional change associated with polarity reversals (Table 1). The observed duration is consistent with the premise that excursions involve short-lived reversal of the field generated in the outer core which has timescales of 500 years or less [*Gubbins*, 1999]. In this scenario, a long-lasting change of polarity occurs in the unusual case where the reversed field in the outer core persists for sufficient time (3–5 kyr) for diffusion of the polarity reversal through the inner core.

[28] Some paleointensity lows at Sites 983/984 (Figure 13) are not associated with directional excursions. These paleointensity lows may, in the future, be found to be associated with directional excursions as higher-resolution sedimentary records become available. A picture is emerging in which geomagnetic directional excursions are often associated with the paleointensity lows that are frequently observed within polarity chrons. The excursional record is often lost due to low sediment accumulation rates, finite remanence lock-in zones, the stochastic nature of sediment accumulation, and/or overprinting of excursional directions by the postexcursional field. Short subchrons with durations of a few thousand years are likely to be found only by continuous sampling of high accumulation rate sedimentary records.

[29] **Acknowledgments.** This research has been supported by the U.S. National Science Foundation (EAR-98-04711). We are grateful to John King for reviewing of this manuscript and to Carlo Laj and Catherine Kissel for discussions and assistance. We are indebted to the staff of the Ocean Drilling Program (ODP) for facilitating this study, and we particularly appreciate the assistance of the staff at the ODP Bremen Core Repository. LSCE contribution 0765.

References

Abrahamsen, N., and W. Sager, Cobb Mountain geomagnetic polarity event and transitions in three deep-sea sediment cores from the Lau Basin, *Proc. Ocean Drill. Program Sci. Results*, *135*, 737–762, 1994.

Baksi, A. K., K. A. Hoffman, and M. McWilliams, Testing the accuracy of the geomagnetic polarity time-scale (GPTS) at 0–5 Ma utilizing $^{40}Ar/^{39}Ar$ incremental heating data on whole-rock basalts, *Earth Planet. Sci. Lett.*, *118*, 135–144, 1993.

Berger, A., and M. F. Loutre, Insolation values for the climate of the last 10 million years, *Quat. Sci. Rev.*, *10*, 297–317, 1991.

Bogue, S. W., Geomagnetic field behavior before and after the Kauai reverse-normal polarity transition, *J. Geophys. Res.*, *106*, 447–461, 2001.

Cande, S. C., and D. V. Kent, A new geomagnetic polarity timescale for the late Cretaceous and Cenozoic, *J. Geophys. Res.*, *97*, 13,917–13,951, 1992.

Champion, D. E., M. A. Lanphere, and M. A. Kuntz, Evidence for a new geomagnetic reversal from lava flows in Idaho: Discussion of short polarity reversals in the Brunhes and late Matuyama polarity chrons, *J. Geophys. Res.*, *93*, 11,667–11,680, 1988.

Channell, J. E. T., Geomagnetic paleointensity and directional secular variation at Ocean Drilling Program (ODP) Site 984 (Bjorn Drift) since 500 ka: Comparisons with ODP Site 983 (Gardar Drift), *J. Geophys. Res.*, *104*, 22,937–22,951, 1999.

Channell, J. E. T., and H. F. Kleiven, Geomagnetic palaeointensities and astrochronological ages for the Matuyama-Brunhes boundary and the boundaries of the Jaramillo Subchron: Palaeomagnetic and oxygen isotope records from ODP Site 983, *Philos. Trans. R. Soc. London, Ser. A*, *358*, 1027–1047, 2000.

Channell, J. E. T., and B. Lehman, The last two geomagnetic polarity reversals recorded in high-deposition-rate sediment drifts, *Nature*, *389*, 712–715, 1997.

Channell, J. E. T., and B. Lehman, Magnetic stratigraphy of Leg 162 North Atlantic Sites 980–984, *Proc. Ocean Drill. Program Sci. Results*, *162*, 113–130, 1999.

Channell, J. E. T., D. A. Hodell, and B. Lehman, Relative geomagnetic paleointensity and ^{18}O at ODP Site 983 (Gardar Drift, North Atlantic) since 350 ka, *Earth Planet. Sci. Lett.*, *153*, 103–118, 1997.

Channell, J. E. T., D. A. Hodell, J. McManus, and B. Lehman, Orbital modulation of geomagnetic paleointensity, *Nature*, *394*, 464–468, 1998.

Chauvin, A., P. Roperch, and R. A. Duncan, Records of geomagnetic reversals from volcanic islands of French Polynesia, 2, Paleomagnetic study of a flow sequence (1.2 to 0.6 Ma) from the Island of Tahiti and discussion of reversal models, *J. Geophys. Res.*, *95*, 2727–2752, 1990.

Clement, B. M., and D. V. Kent, Short polarity intervals within the Matuyama: Transition field records from hydraulic piston cored sediments from the North Atlantic, *Earth Planet. Sci. Lett.*, *81*, 253–264, 1987.

Clement, B. M., and D. G. Martinson, A quantitative comparison of two paleomagnetic records of the Cobb Mountain Subchron from North Atlantic deep-sea sediments, *J. Geophys. Res.*, *97*, 1735–1752, 1992.

Clement, B. M., and R. Robinson, The magnetostratigraphy of Leg 94 sediments, *Initial Rep. Deep Sea Drill. Proj.*, *94*, 635–650, 1987.

Doell, R. R., and G. B. Dalrymple, Geomagnetic polarity epochs: A new polarity event and the age of the Brunhes-Matuyama boundary, *Science*, *152*, 1060–1061, 1966.

Flower, B. P., D. W. Oppo, J. F. McManus, K. A. Venz, D. A. Hodell, and J. A. Cullen, North Atlantic intermediate to deep water circulation and chemical stratification during the past 1 Myr, *Paleoceanography*, *15*, 388–403, 2000.

Grommé, C. S., and R. L. Hay, Magnetization of basalt of Bed I, Olduvai Gorge, *Nature*, *200*, 560–561, 1963.

Grommé, C. S., and R. L. Hay, Geomagnetic polarity epochs: Age and duration of the Olduvai normal polarity event, *Earth Planet. Sci. Lett.*, *18*, 179–185, 1971.

Gubbins, D., The distinction between geomagnetic excursions and reversals, *Geophys. J. Int.*, *137*, F1–F3, 1999.

Guyodo, Y., C. Richter, and J.-P. Valet, Paleointensity record from Pleistocene sediments (1.4-0 Ma) off the California Margin, *J. Geophys, Res.*, *104*, 22,953–22,964, 1999.

Heirtzler, J. R., G. O. Dickson, E. M. Herron, W. C. Pittman III, and X. LePichon, Marine magnetic anomalies, geomagnetic field reversal and motions of the ocean floor and continents, *J. Geophys. Res,.*, *73*, 2119–2136, 1968.

Hsu, V., D. L. Merrill, and H. Shibuya, Paleomagnetic transition records of the Cobb Mountain event from sediment of the Celebes and Sulu seas, *Geophys. Res. Lett.*, *17*, 2069–2072, 1990.

Izett, G. A., and J. D. Obradovich, $^{40}Ar/^{39}Ar$ age constraints for the Jaramillo normal subchron and the Matuyama-Brunhes geomagnetic boundary, *J. Geophys. Res.*, *99*, 2925–2934, 1994.

Kent, D. V., and D. J. Spariosu, High resolution magnetostratigraphy of Caribbean Plio-Pleistocene sediments, *Palaeogeogr. Palaeoclimatol. Palaeoecol.*, *42*, 47–64, 1983.

King, J. W., S. K. Banerjee, and J. Marvin, A new rock-magnetic approach to selecting sediments for geomagnetic paleointensity studies: Application to paleointensity for the last 4000 years, *J. Geophys. Res.*, *88*, 5911–5921, 1983.

Kirschvink, J. L., The least squares lines and plane analysis of paleomagnetic data, *Geophys. J.R. Astron. Soc.*, *62*, 699–718, 1980.

Kok, Y. S., and L. Tauxe, A relative geomagnetic paleointensity stack from Ontong-Java Plateau sediments for the Matuyama, *J. Geophys. Res.*, *104*, 25,401–25,413, 1999.

Lourens, L. J., A. Antonarakou, F. J. Hilgen, A. A. M. Van Hoof, C. Vergnaud-Grazzini, and W. J. Zachariasse, Evaluation of the Plio-Pleistocene astronomical timescale, *Paleoceanography*, *11*, 391–413, 1996.

Mankinen, E. A., and C. S. Gromme, Paleomagnetic data from the Cosa Range, California, and current status of the Cobb Mountain normal geomagnetic polarity event, *Geophys. Res. Lett.*, *9*, 1239–1282, 1982.

Mankinen, E. A., J. M. Donnelly, and C. S. Gromme, Geomagnetic polarity event recorded at 1.1 m.y.B.P. on Cobb Mountain, Clear Lake Volcanic Field, California, *Geology*, *6*, 653–656, 1978.

Manley, P. L., and D. W. Caress, Mudwaves on the Gardar Sediment Drift, NE Atlantic, *Paleoceanography*, *9*, 973–988, 1994.

Mazaud, A., and J. E. T. Channell, The top Olduvai polarity transition at ODP Site 983 (Iceland Basin), *Earth Planet. Sci. Lett.*, *166*, 1–13, 1999.

McCave, I. N., P. F. Lonsdale, C. D. Hollister, and W. D. Gardner, Sediment transport over the Hatton and Gardar contourite drifts, *J. Sediment. Petrol.*, *50*, 1049–1062, 1980.

McDougall, I., and J. Wensink, Paleomagnetism and geochronology of the Pliocene-Pleistocene lavas in Iceland, *Earth Planet. Sci. Lett.*, *1*, 232–236, 1966.

McFadden, P. L., R. T. Merrill, and M. W. McElhinny, Dipole/quadrupole family modelling of paleosecular variation, *J. Geophys. Res.*, *93*, 11,583–11,588, 1988.

McIntyre, K., A. C. Ravelo, and M. L. Delaney, North Atlantic intermediate waters in the late Pliocene to early Pleistocene, *Paleoceanography*, *14*, 324–335, 1999.

McManus, J., D. W. Oppo, and J. L. Cullen, A 0.5-million-year record of millennial-scale climate variability in the North Atlantic, *Science*, *283*, 971–974, 1999.

Meynadier, L., J.-P. Valet, C. Bassinot, N. J. Shackleton, and Y. Guyodo, Asymmetrical saw-tooth pattern of the geomagnetic field intensity from equatorial sediments in the Pacific and Indian Oceans, *Earth Planet. Sci. Lett.*, *126*, 109–127, 1994.

Oppo, D. W., J. F. McManus, and J. L. Cullen, Abrupt climate events 500,000–340,000 years ago: Evidence from subpolar North Atlantic sediments, *Science*, *279*, 1335–1338, 1998.

Ortiz, J., A. Mix, S. Harris, and S. O'Connell, Diffuse spectral reflectance as a proxy for percent carbonate content in North Atlantic sediments, *Paleoceanography*, *14*, 171–186, 1999.

Raymo, M. E., W. F. Ruddiman, J. Backman, B. M. Clement, and D. G. Martinson, Late Pliocene variation in Northern Hemisphere ice sheets and North Atlantic deep water circulation, *Paleoceanography*, *4*, 413–446, 1989.

Raymo, M. E., K. Ganley, S. Carter, D. W. Oppo, and J. McManus, Millennial-scale climate instability during the early Pleistocene epoch, *Nature*, *392*, 699–702, 1998.

Ruddiman, W. F., M. E. Raymo, D. G. Martinson, B. M. Clement, and J. Backman, Pleistocene evolution: Northern Hemisphere ice sheet and North Atlantic Ocean, *Paleoceanography*, *4*, 353–412, 1989.

Shackleton, N. J., et al., Oxygen isotope calibration of the onset of ice-rafting and history of glaciation in the North Atlantic region, *Nature*, *307*, 620–623, 1984.

Shackleton, N. J., A. Berger, and W. R. Peltier, An alternative astronomical calibration of the lower Pleistocene timescale based on ODP Site 677, *Trans. R. Soc. Edinburgh Earth Sci.*, *81*, 251–261, 1990.

Shackleton, N. J., S. Crowhurst, T. Hagelberg, N. G. Pisias, and D. A. Schneider, A new late Neogene time scale: Application to Leg 138 sites, *Proc. Ocean Drill. Program Sci. Results*, *138*, 73–101, 1995.

Shipboard Scientific Party, Site 983, *Proc. Ocean Drill. Program Initial Rep.*, *162*, 139–167, 1996a.

Shipboard Scientific Party, Site 984, *Proc. Ocean Drill. Program Initial Rep.*, *162*, 169–222, 1996b.

Singer, B. S., K. A. Hoffman, A. Chauvin, R. S. Coe, and M. S. Pringle, Dating transitionally magnetized lavas of the late Matuyama Chron: Toward a new $^{40}Ar/^{39}Ar$ timescale of reversals and events, *J. Geophys. Res.*, *104*, 679–693, 1999.

Spell, T. L., and I. McDougall, Revisions to the age of the Brunhes/Matuyama boundary and the Pleistocene geomagnetic polarity timescale, *Geophys. Res. Lett.*, *19*, 1182–1184, 1992.

Takatsugi, K. O., and M. Hyodo, A geomagnetic excursion during the late Matuyama Chron, the Osaka group, southwest Japan, *Earth Planet. Sci. Lett.*, *136*, 511–524, 1995.

Tauxe, L., Sedimentary records of relative paleointensity of the geomagnetic field: Theory and practice, *Rev. Geophys.*, *31*, 319–354, 1993.

Tauxe, L., J. L. LaBrecque, R. Dodson, and M. Fuller, U-channels—A new technique for paleomagnetic analysis of hydraulic piston cores, *Eos Trans. AGU*, *64*, 219, 1983.

Tiedemann, R., M. Sarnthein, and N. J. Shackleton, Astronomic timescale for the Pliocene Atlantic $d^{18}O$ and dust flux records of Ocean Drilling Program Site 659, *Paleoceanography*, *9*, 619–638, 1994.

Turrin, B. D., J. M. Donnelly-Nolan, and B. C. Hearn Jr., $^{40}Ar/^{39}Ar$ ages from the rhyolite of Alder Creek, California: Age of the Cobb Mountain normal polarity subchron revisited, *Geology*, *22*, 251–254, 1994.

Valet, J. P., and L. Meynadier, Geomagnetic field intensity and reversals during the past four million years, *Nature*, *366*, 234–238, 1993.

Vandamme, D., A new method to determine paleosecular variation, *Phys. Earth Planet. Inter.*, *85*, 131–142, 1994.

Venz, K. A., D. A. Hodell, C. Stanton, and D. A. Warnke, A 1.0 Myr record of glacial North Atlantic Intermediate Water variability from ODP Site 982 in the northeast Atlantic, *Paleoceanography*, *14*, 42–52, 1999.

Watkins, N. D., I. McDougall, and L. Kristjansson, A detailed paleomagnetic survey of the type location for the Gilsa geomagnetic polarity event, *Earth Planet. Sci. Lett.*, *27*, 436–444, 1975.

Weeks, R., C. Laj, L. Endignoux, M. Fuller, A. Roberts, R. Manganne, E. Blanchard, and W. Goree, Improvements in long-core measurement techniques: Applications in palaeomagnetism and palaeoceanography, *Geophys. J. Int.*, *114*, 651–662, 1993.

Yang, Z., B. M. Clement, G. D. Acton, S. P. Lund, M. Okada, and T. Williams, Records of the Cobb Mountain Subchron from the Bermuda Rise (ODP Leg 172), *Earth Planet. Sci. Lett.*, *193*, 303–313, 2001.

J. E. T. Channell, P. Sullivan, and S. Turner, Department of Geological Sciences, University of Florida, P.O. Box 112120, Gainesville, FL 32611-2120, USA. (jetc@nersp.nerdc.ufl.edu)

A. Mazaud, Laboratoire des Sciences du Climat et de l'Environnement, Ave Terrasse, Cedex, F-91198 Gif-sur-Yvette, France. (mazaud@lsce.cnrs-gif.fr)

M. E. Raymo, Department of Earth Sciences, Boston University, 685 Commonwealth Avenue, Boston, MA 02215, USA. (raymo@mit.edu)

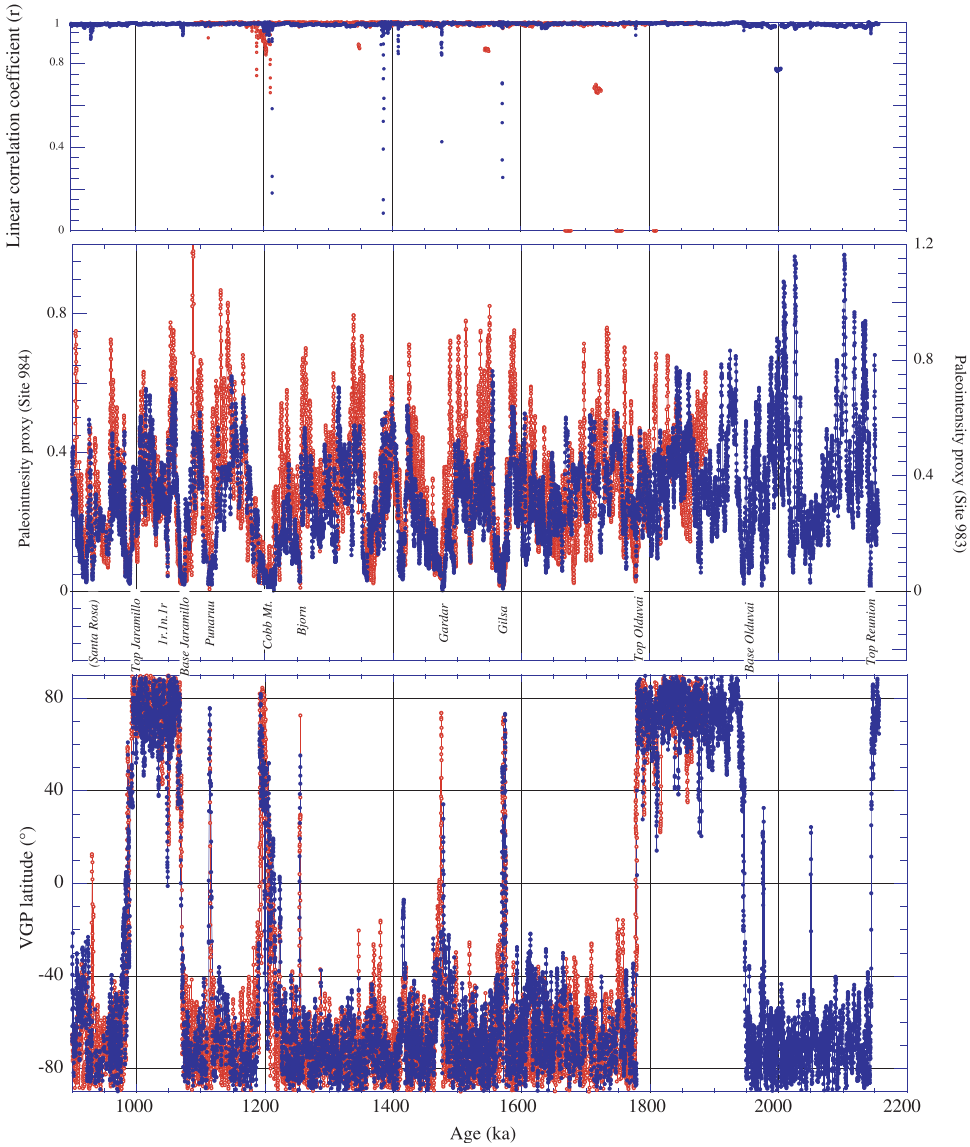

Figure 13. Site 983 (open symbols) and Site 984 (solid symbols) paleointensity proxy based on the slope of the NRM/ARM plot in the 30–60 mT peak demagnetization interval. The linear correlation coefficient (*r*) indicates the linearity of the NRM/ARM plot in this demagnetization interval. The virtual geomagnetic polar (VGP) latitudes show polarity reversals and geomagnetic excursions (defined here as VGP latitudes which cross the virtual geomagnetic equator) relative to the paleointensity record.

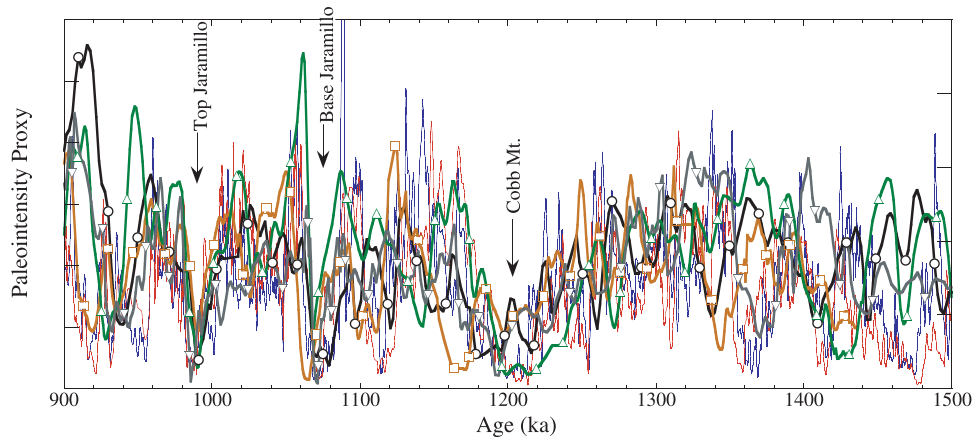

Figure 15. Comparison of the Site 983/984 paleointensity records (smoothed with a 10-point running mean, thin lines) with other published paleointensity records (thick lines). Triangles, Ontong-Java Plateau [*Kok and Tauxe*, 1999]; inverted triangles, equatorial Pacific [*Valet and Meynadier*, 1993]; open circles, equatorial Indian Ocean [*Meynadier et al.*, 1994]; open squares, California Margin [*Guyodo et al.*, 1999].